GFAP (1:1000, Chemicon, Billerica, MA) was used as a specific marker for astrocytes, and monoclonal antibodies to HLA-DR, DP, DQ (1:100, Dako, Glostrup, Denmark) were used as markers for microglia. Monoclonal antibodies 82E1 (diluted 1:500, IBL, Gunma, Japan) and AT8 (1:5000, Innogenetics, Gent, Belgium) were used to detect Aβ in SPs and phosphorylated tau in NFTs, respectively. For immunostaining of Aβ, the sections were pretreated with 100% formic acid (Wako, Osaka, Japan) for 30 sec before the blocking procedure.

For immunofluorescence staining, sections were blocked with skim milk. After they were incubated with mixed primary antibodies for 48 hr at 4°C, the following secondary antibodies were used: first, fluorescein isothiocyanate-conjugated donkey anti-rabbit IgG antibody (1: 1000, Jackson Immuno Research, West Grove, PA) for 2 hr at room temperature, and then biotinylated donkey anti-mouse IgG antibody (1: 1000, Jackson Immuno Research) for 2 hr at room temperature. The biotinylated secondary antibody treatment was followed by incubation with Texas-Red dye-conjugated streptavidin (1:1000, Jackson Immuno Research) for 1 hr at room temperature.

Primary culture of cerebral neuronal cells. Primary cerebral neuronal cells were prepared from the cerebri of 16.5-day-old embryos of wild-type and mPGES-$1^{-/-}$ mice using Nerve-Cell Culture System (Sumitomo Bakelite, Tokyo, Japan). In brief, cerebral tissues were cleaned of meninges, minced, and treated with protease mixure. After mechanical dissociation by pipetting and treatment with dissociation solution, we resuspended cells in nerve cell culture medium, and then plated onto poly-L-lysine-coated plates or glass dishes (Φ 35 mm) at a density of 2.4 x 10^6 cells/well. After 7 days of the culture, we used neuronal cells to examine the effects of $A\beta_{31\text{-}35}$

(Peptide Institute, Inc., Osaka, Japan) on the expression of mPGES-1 and the cell death. The viable cells were peeled off by pipetting and counted using the trypan blue exclusion method. Neuronal cell identity was confirmed by immunostaining with the neuron marker anti-MAP-2 (Sigma) and astrocyte marker anti-GFAP antibodies (Chemicon).

RT-PCR analysis. Total RNA was extracted from mouse primary cerebral neuronal cells using Trizol Reagent (Invitrogen). Synthesis of cDNA was performed with 2 μg of the total RNA isolated from mouse primary cerebral neuronal cells, oligo dT primers, and SuperScript III Reverse Transcriptase (Invitrogen). Subsequent amplifications of the partial cDNA fragments were performed by Ex-Taq Polymerase (TaKaRa) using the reverse-transcribed products as a template with a set of specific oligonucleotide primers as follows: mPGES-1 sense 5'-AATGGGAGACGGAGCCATGA-3' and antisense 5'-ACCAGTCACGTGTCTCTCCT-3'; COX-2 sense 5'-GGTCTGGTGCCTGGTCTGATGATG-3' and antisense 5'-GTCCTTCAAGGAGAATGGTGC-3'; GAPDH sense 5'-TCGTGGATCTGACGTGCCGCCTG-3' and antisense 5'-CACCACCCTGTTGCTGTAGCCGTAT. The PCR mixtures were subjected to 35 (for mPGES-1 and COX-2) or 25 (for GAPDH) cycles of amplification by denaturation (45 s at 94°C), annealing (60 s at 60°C) and elongation (60 s at 72°C). The PCR products were analyzed by 1% agarose gel electrophoresis with ethidium bromide.

TUNEL staining experiments. The TUNEL staining experiments were performed as previously described (39). Briefly, after the treatment of $A\beta_{31\text{-}35}$ and/or PGE_2, the cells were fixed for 25 min in 4% paraformaldehyde in PBS, permeabilized for 5 min in 0.2% Triton X-100, and

then stained by using the DeadEnd Fluorometric TUNEL system (Promega) according to the manufacturer's instructions. For the positive control experiments, the cells were treated with DNase I (TaKaRa, Japan) for 10 min before the staining. Three randomly chosen microscopic fields were captured, and the numbers of TUNEL-positive neuronal nuclei were calculated.

Water Maze. Morris water-maze tests were performed to evaluate learning ability at the age of 10 to 11 months. The apparatus used in the tests consisted of a blue plastic circular pool 100 cm diameter enclosed by a 25-cm high wall. The pool was filled with water kept at a temperature of 19°C. A transparent plastic platform (8 cm in diameter) was placed 0.5 cm below the water surface and 18 cm from the wall of the pool. Visual cues for navigation were provided by four posters on the room wall.

In training trials for the Morris water-maze test, a mouse was placed at an area opposite the platform set in the pool and allowed to swim. The behavior was recorded by video. The time required to reach the platform (the latency period) and the distance of swimming were measured by using the analysis software. Such training trials were repeated for 5 days (3 trials/day). The starting point was randomly selected from three points.

A probe trial of the Morris water-maze test was performed on the day after the 5-day training was finished. The probe test was performed without the platform. The mouse was placed in the pool and swam for 60 s looking for a platform. The proportion of time spent in the different quadrants was recorded.

ACKNOWLEDGMENTS. We are grateful to all patients and their bereaved family members

who kindly gave their informed consent for enrollment in this study. This work was supported in part by Grants-in-Aid for Comprehensive Research on Aging and Health, and Research on Dementia from the Ministry of Health, Labour and Welfare of Japan, Grants-in-Aid for Scientific Research and "High-Tech Research Center" Project for Private Universities (matching fund subsidy (2004-2007)) from the Ministry of Education, Science, Culture, Sports and Technology of Japan, and a Showa University Special Grant-in-Aid for Innovative Collaborative Research Projects. D. Kamei was supported by Research Fellowships of the Japan Society for the Promotion of Science for Young Scientists.

References

1. Selkoe DJ (2001) Alzheimer's disease: genes, proteins, and therapy. *Physiol Rev* 81:741-766.
2. McGeer PL, McGeer EG (2007) NSAIDs and Alzheimer disease: epidemiological, animal model and clinical studies. *Neurobiol Aging* 28:639-647.
3. Townsend KP, Praticò D (2005) Novel therapeutic opportunities for Alzheimer's disease: focus on nonsteroidal anti-inflammatory drugs. *FASEB J* 19:1592-1601.
4. Akiyama H, et al. (2000) Inflammation and Alzheimer's disease. *Neurobiol Aging* 21:383-421.
5. Praticò D, Trojanowski JQ (2000) Inflammatory hypotheses: novel mechanisms of Alzheimer's neurodegeneration and new therapeutic target? *Neurobiol Aging* 21:441-445.
6. Lim GP, et al. (2000) Ibuprofen suppresses plaque pathology and inflammation in a mouse model for Alzheimer's disease. *J Neurosci* 20:5709-5714.

7. Yan Q, et al. (2003) Anti-inflammatory drug therapy alters β-amyloid processing and deposition in an animal model of Alzheimer's disease. *J Neurosci* 23:7504-7509.

8. Smith WL, Meade EA, DeWitt DL (1994) Interactions of PGH synthase isozymes-1 and -2 with NSAIDs. *Ann NY Acad Sci* 744:50-57.

9. Pasinetti GM, Aisen PS (1998) Cyclooxygenase-2 expression is increased in frontal cortex of Alzheimer's disease. *Neuroscience* 87:319-324.

10. Ho L, et al. (1999) Regional distribution of cyclooxygenase-2 in the hippocampal formation in Alzheimer's disease. *J Neurosci Res* 57:295-303.

11. Oka A, Takashima S (1997) Induction of cyclo-oxygenase 2 in brains of patients with Down's syndrome and dementia of Alzheimer type: specific localization in affected neurons and axons. *Neuroreport* 8:1161-1164.

12. Yasojima K, Schwab C, McGeer EG, McGeer PL (1999) Distribution of cyclooxygenase-1 and cyclooxygenase-2 mRNAs and proteins in human brain and peripheral organs. *Brain Res* 830:226-236.

13. Fujimi K, et al. (2007) Altered expression of COX-2 in subdivisions of the hippocampus during aging and in Alzheimer's disease: the Hisayama study. *Dement Geriatr Cogn Disord* 23:423-431.

14. Montine TJ, et al. (1999) Elevated CSF prostaglandin E_2 levels in patients with probable AD. *Neurology* 53:1495-1498.

15. Murakami M, Kudo I (2004) Recent advances in molecular biology and physiology of the prostaglandin E_2-biosynthetic pathway. *Prog Lipid Res* 43:3-35.

16. Murakami M, et al. (2000) Regulation of prostaglandin E_2 biosynthesis by inducible membrane-associated prostaglandin E_2 synthase that acts in concert with cyclooxygenase-2. *J Biol Chem* 275:32783-32792.

17. Stichtenoth DO, et al. (2001) Microsomal prostaglandin E synthase is regulated by proinflammatory cytokines and glucocorticoids in primary rheumatoid synovial cells. *J Immunol* 167:469-474.

18. Samuelsson B, Morgenstern R, Jakobsson PJ (2007) Membrane prostaglandin E synthase-1: a novel therapeutic target. *Pharmacol Rev* 59:207-224.

19. Satoh K, et al. (2000) Expression of prostaglandin E synthase mRNA is induced in beta-amyloid treated astrocytes. *Neurosci Lett* 283:221-223.

20. Hsiao K, et al. (1996) Correlative memory deficits, Aβ elevation, and amyloid plaques in transgenic mice. *Science* 274:99-102.

21. Kamei D, et al. (2004) Reduced pain hypersensitivity and inflammation in mice lacking microsomal prostaglandin E synthase-1. *J Biol Chem* 279:33684-33695.

22. Kamei D, et al. Microsomal prostaglandin E synthase-1 in both cancer cells and hosts contributes to tumor growth, invasion and metastasis. *Biochem J* in press?.

23. Misiti F, et al. (2005) Aβ(31-35) peptide induce apoptosis in PC 12 cells: contrast with Aβ(25-35) peptide and examination of underlying mechanisms. *Neurochem Int* 46:575-583.

24. Misiti F, et al. A crucial role for the redox state of methionine-35 residue. *Neurochem Int* 49:525-532.

25. Yan XZ, Qiano JT, Dou Y, Qiao ZD (1999) β-amyloid peptide fragment 31-35 induces

apoptosis in cultured cortical neurons. *Neuroscience* 92:177-184.

26. Behl C, Davis JB, Lesley R, Schubert D (1994) Hydrogen peroxide mediates amyloid β protein toxicity. *Cell* 77:817-827.

27. Sandee D, Sivanuntakorn S, Vichai V, Kramyu J, Kirtikara K (2009) Up-regulation of microsomal prostaglandin E synthase-1 in COX-1 and COX-2 knock-out mouse fibroblast cell lines. *Prostaglandins Other Lipid Mediat* 88:111-116.

28. Yermakova AV, O'Banion MK (2001) Downregulation of neuronal cyclooxygenase-2 expression in end stage Alzheimer's disease. *Neurobiol Aging* 22:823-386.

29. Chaudhry UA, Zhuang H, Crain BJ, Doré S (2008) Elevated microsomal prostaglandin-E synthase-1 in Alzheimer's disease. *Alzheimers Dement* 4:6-13.

30. Sugimoto Y, Narumiya S (2007) Prostaglandin E receptors. *J Biol Chem* 282:11613-11617.

31. Shie FS, Breyer RM, Montine TJ (2005) Microglia lacking E prostanoid receptor subtype 2 have enhanced Aβ phagocytosis yet lack Aβ-activated neurotoxicity. *Am J Pathol* 166:1163-1172.

32. Liang X, et al. (2005) Deletion of the prostaglandin E_2 EP2 receptor reduces oxidative damage and amyloid burden in a model of Alzheimer's disease. *J Neurosci* 25:10180-10187.

33. Echeverria V, Clerman A, Doré S (2005) Stimulation of PGE_2 receptors EP2 and EP4 protects cultured neurons againsat oxidative stress and cell death following β-amyloid exposure. *Eur J Neurosci* 22:2199-2206.

34. Takadera T, Shiraishi Y, Ohyashiki T (2004) Prostaglandin E_2 induced caspase-dependent apoptosis possibly through activation of EP2 receptors in cultured hippocampal neurons.

Neurochem Lett 45:713-719.

35. Sanchez-Mejia RO, et al. (2008) Phospholipase A_2 reduction ameliorates cognitive deficits in a mouse model of Alzheimer's disease. *Nat Neurosci* 11:1311–1318.

36. El Khoury J, Luster AD (2008) Mechanisms of microglia accumulation in Alzheimer's disease: therapeutic implications. *Trends Phamacol Sci* 29:626-632.

37. Hickman SE, Allison EK, El Khoury J (2008) Microglial dysfunction and defective beta-amyloid clearance pathways in aging Alzheimer's disease mice. *J Neurosci* 28:8354-8360.

38. Hoshino T, et al. (2007) Involvement of prostaglandin E_2 in production of amyloid-β peptides both *in vitro* and *in vivo*. *J Biol Chem* 282:32676-32688.

39. Zhang H, et al. (2008) Full length mutant huntington is required for altered Ca^{2+} signaling and apoptosis of striatal neurons in the YAC mouse model of Huntington's disease. *Neurobiol Dis* 31:80-88.

FIGURE LEGENDS

Fig. 1. High expression of mPGES-1 in brains of human AD (A – C) and Tg2576 mice (D – F). (A) Representative images of anti-mPGES-1-stained sections in CA2-3 region of the hippocampus from NC (Left) and AD (Right). (B) Values along the vertical axis of quantitative analysis graphs represent total pixel counts. *, $P < 0.05$ by Dunnett's two-tailed test (vs. NC). (C) Double immunostaninig with anti-mPGES-1 and AT-8 antibodies. AT-8 positive, dark purple; mPGES-1-positive, brown. (D) Representative images of anti-mPGES-1-stained sections in the

brain from control wild-type (Left) and Tg2576 mice (Right). (E) Double-immunostaining of mPGES-1 expression (brown) associated with Aβ plaques (dark purple). (F) Double-immunofluorescent staining with anti-mPGES-1 and anti-GFAP antibodies. Immunofluorescent staining of cells for mPGES-1 expressions (green), anti-GFAP antibody staining of reactive astrocytes (red) and the merged image.

Fig. 2. Induction of mPGES-1 expression and PGE_2 production in Aβ-treated mouse cerebri neuronal cells. (A) RT-PCR analysis for mPGES-1 expression in neuronal cells. RNA was prepared from neuronal cells cultured with or without Aβ for the indicated times, and then RT-PCR analysis for mPGES-1, COX-2 and GAPDH (as a control) were performed. (B) Immunocytostaining analysis for mPGES-1 expression in neuronal cells. mPGES-1 and GFAP or MAP-2 were double immunostained in neuronal cells cultured with or without Aβ for 72 h. (C) PGE_2 production from neuronal cells. Neuronal cells were prepared from wild-type (Left) and mPGES-1 KO mice (Right), and then cultured with or without Aβ for the indicated times. Amounts of PGE_2 in culture medium from the cultured neuronal cells were assayed with enzyme immunoassay kit. All values are means ± SD for at least 4 independent experiments.

Fig. 3. Effects of mPGES-1 deficiency on changes in cell numbers of Aβ-treated mouse cerebri neuronal cells. (A) Neuronal cells prepared from wild-type (Left) and mPGES-1 KO mice (Right) were cultured with or without Aβ for the indicated times, and the cell numbers were counted. All values are means ± SD for at least 3 independent experiments. (B) GFAP and MAP-2 were double immunostained in wild-type mice- (Left) or mPGES-1 KO mice-derived (Right) neuronal cells cultured with or without Aβ for 72 h.

Fig. 4. Effects of mPGES-1 deficiency on Aβ-induced apoptosis in mouse cerebri neuronal cells. (A) Neuronal cells prepared from wild-type (Left) and mPGES-1 KO mice (Right) were cultured with or without Aβ for 72 h, and the apoptotic cells were TUNEL staining. All values are means ± SD for at least 5 independent experiments. (B) mPGES-1 KO mice-derived neuronal cells were cultured with or without Aβ and PGE_2 for 72 h, and the apoptotic cells were TUNEL staining. All values are means ± SD for at least 3 independent experiments.

Fig. 5. Effects of mPGES-1 deficiency on learning impairments and histopathologic changes in Tg2576 mice. (A) Learning impairments in mPGES-1 deficient Tg2576 mice. Morris water-maze tests were performed using $APPsw^{+/-}$/$mPGES\text{-}1^{+/-}$ (as Tg2576 mice), $APPsw^{+/-}$/$mPGES\text{-}1^{-/-}$ (as mPGES-1 deficient Tg2576 mice), $APPsw^{-/-}$/$mPGES\text{-}1^{+/-}$ (as control mice), and $APPsw^{-/-}$/$mPGES\text{-}1^{-/-}$ mice (as mPGES-1 deficient mice) at the age of 10 to 11 months. The probe test was performed without the platform on the day after the 5-day training was finished. While the mouse swam for 60 s looking for a platform, the proportion of time spent in the different quadrants was recorded. All values are means + SD for at least 3 independent experiments. (B) Histopathologic changes in mPGES-1 deficient Tg2576 mice. Brain tissues were prepared from $APPsw^{+/-}$/$mPGES\text{-}1^{+/-}$ (as Tg2576 mice) and $APPsw^{+/-}$/$mPGES\text{-}1^{-/-}$ (as mPGES-1 deficient Tg2576 mice) at the age of 10 to 11 months. Representative images of anti-mPGES-1, anti-Aβ, anti-GFAP or anti-Iba1-stained sections were shown.

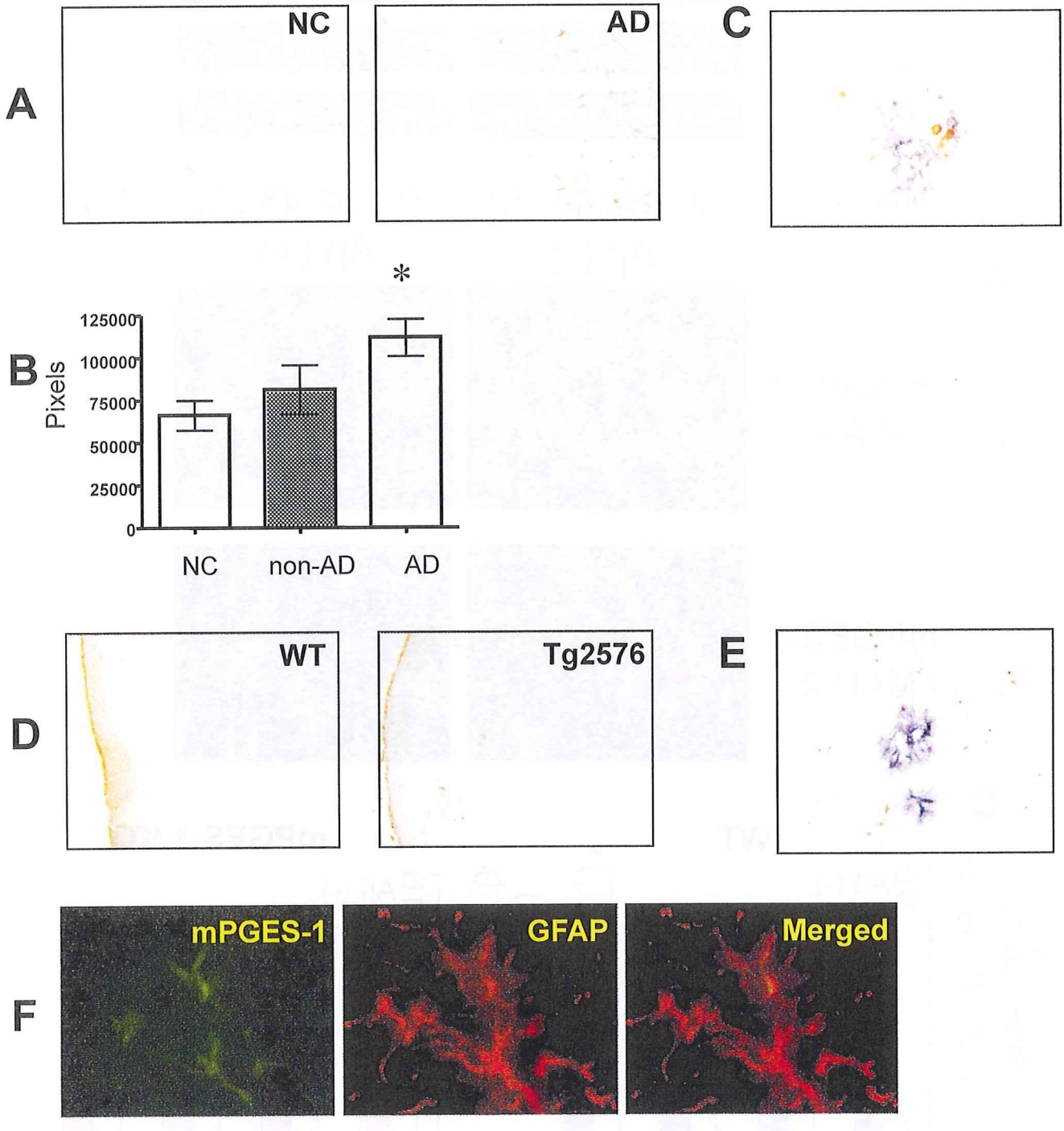
A
NC
AD
C
B
*
Pixels
125000
100000
75000
50000
25000
0
NC
non-AD
AD
D
WT
Tg2576
E
F
mPGES-1
GFAP
Merged

Fig. 1

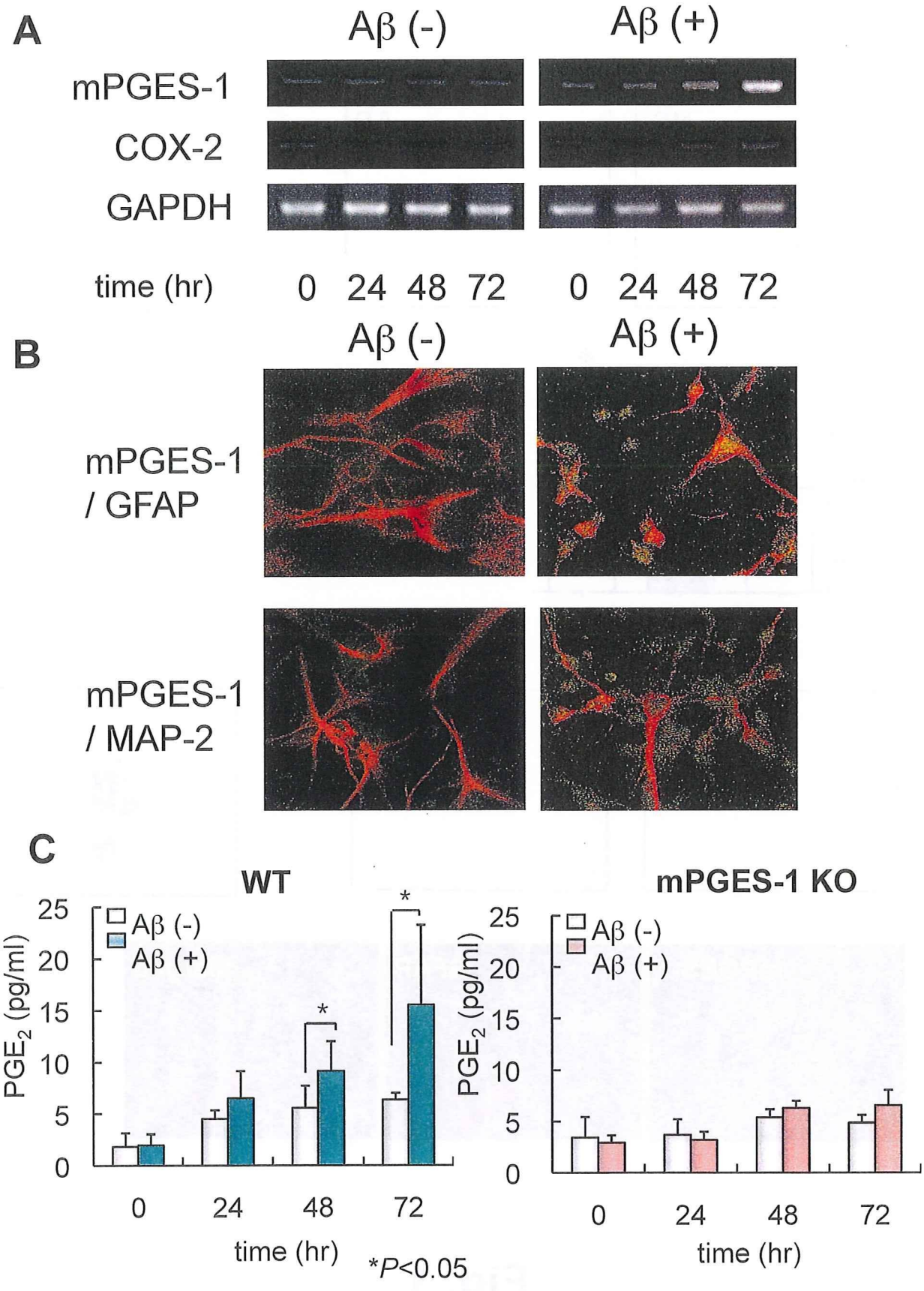
A
Aβ (-)
Aβ (+)
mPGES-1
COX-2
GAPDH
time (hr)
0 24 48 72
0 24 48 72
B
Aβ (-)
Aβ (+)
mPGES-1
/ GFAP
mPGES-1
/ MAP-2
C
WT
mPGES-1 KO
Aβ (-)
Aβ (+)
PGE2 (pg/ml)
25
20
15
10
5
0
0
24
48
72
time (hr)
*
*P<0.05

Fig. 2

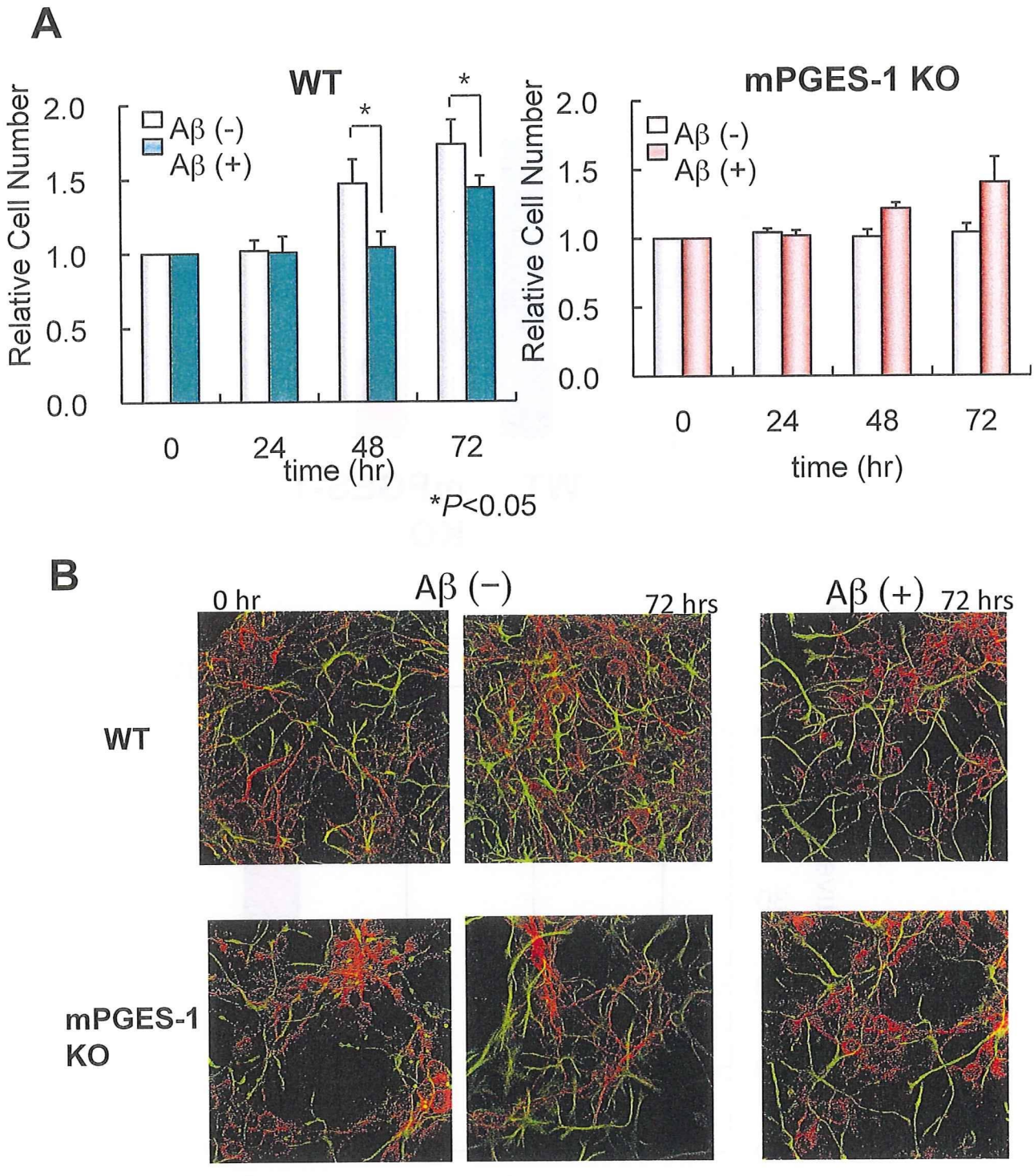
A
WT
mPGES-1 KO
Relative Cell Number
2.0
1.5
1.0
0.5
0.0
Aβ (-)
Aβ (+)
*
0
24
48
72
time (hr)
*P<0.05
B
0 hr
Aβ (−)
72 hrs
Aβ (+)
72 hrs
WT
mPGES-1
KO

Fig. 3

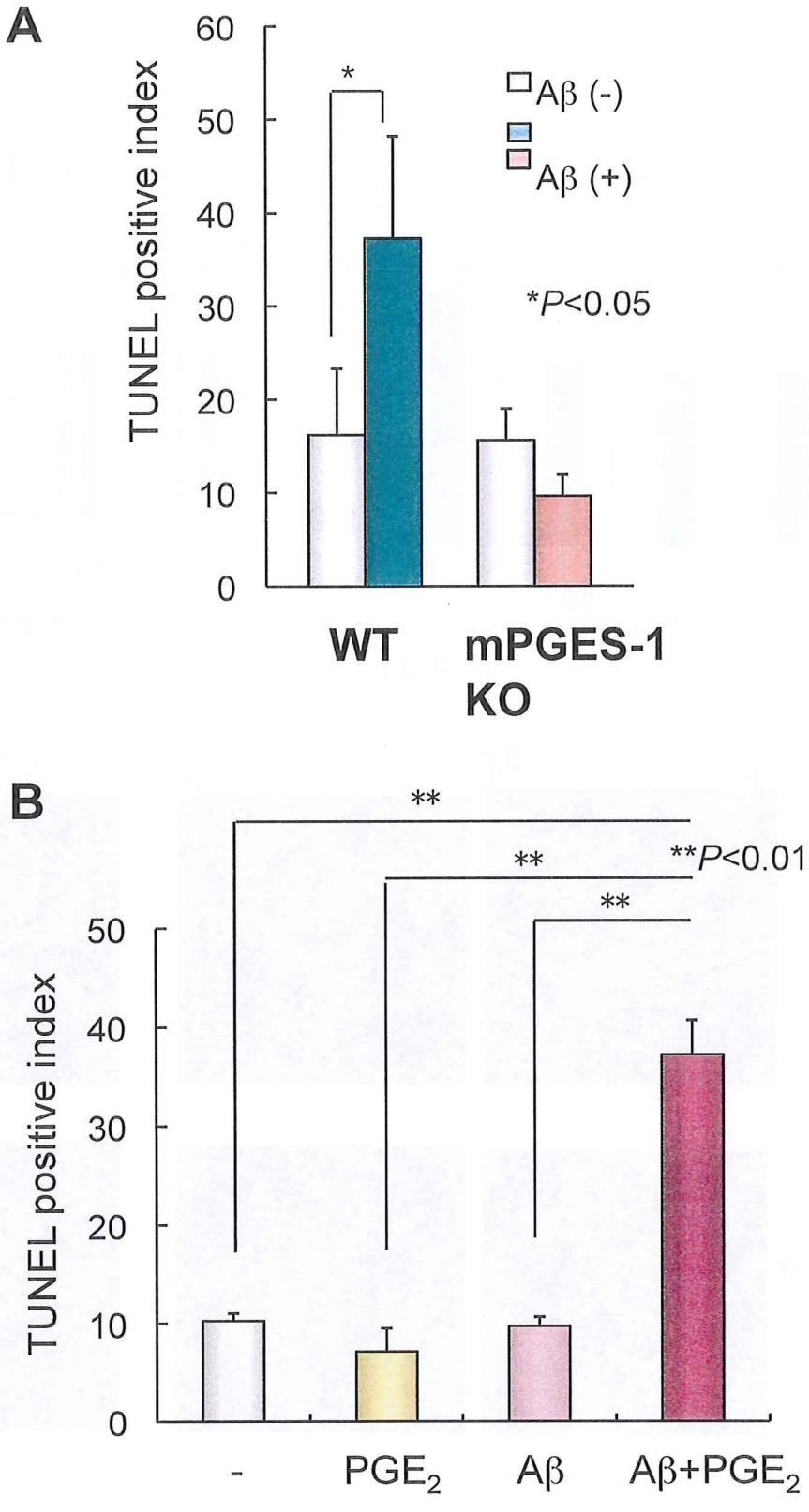
A
TUNEL positive index
60
50
40
30
20
10
0
*
Aβ (-)
Aβ (+)
*P<0.05
WT
mPGES-1 KO
B
**
**
**
**P<0.01
TUNEL positive index
50
40
30
20
10
0
-
PGE2
Aβ
Aβ+PGE2

Fig. 4

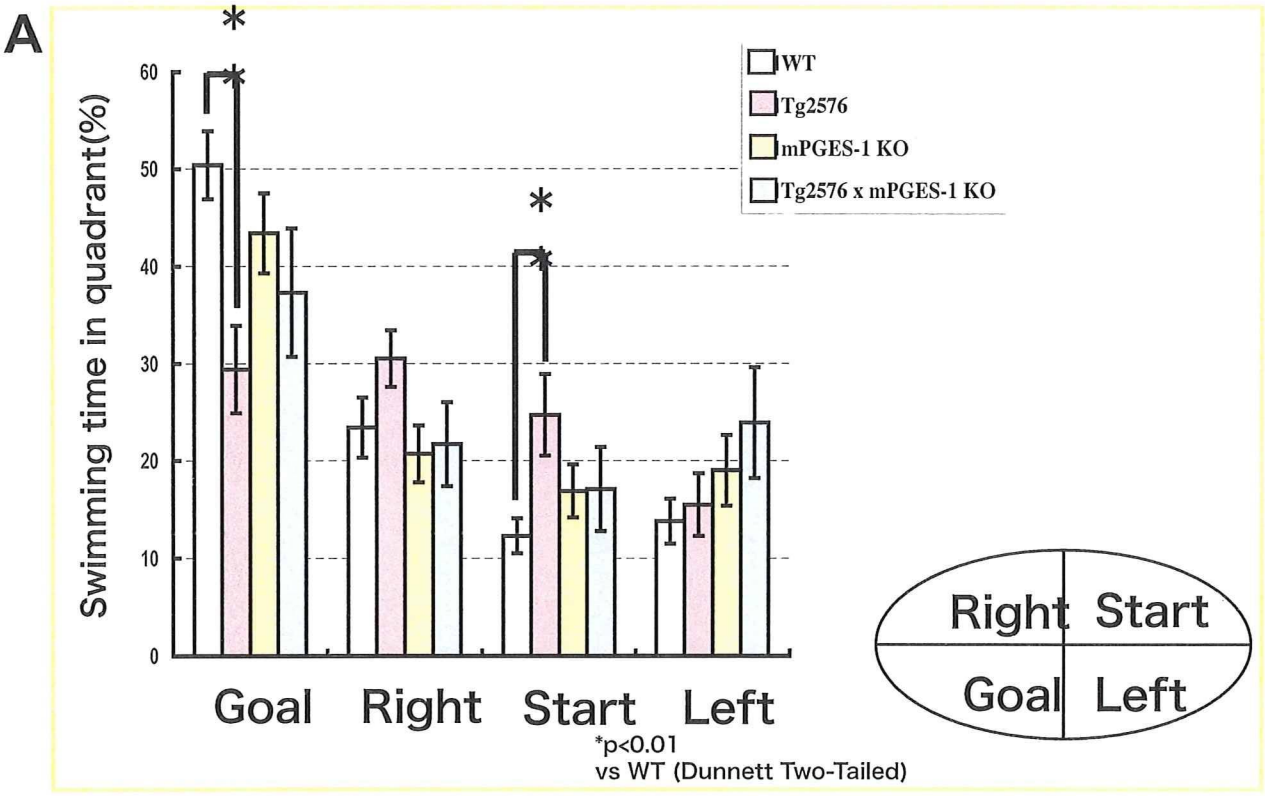
A
Swimming time in quadrant(%)
60
50
40
30
20
10
0
WT
Tg2576
mPGES-1 KO
Tg2576 x mPGES-1 KO
Goal
Right
Start
Left
*p<0.01
vs WT (Dunnett Two-Tailed)
Right Start
Goal Left

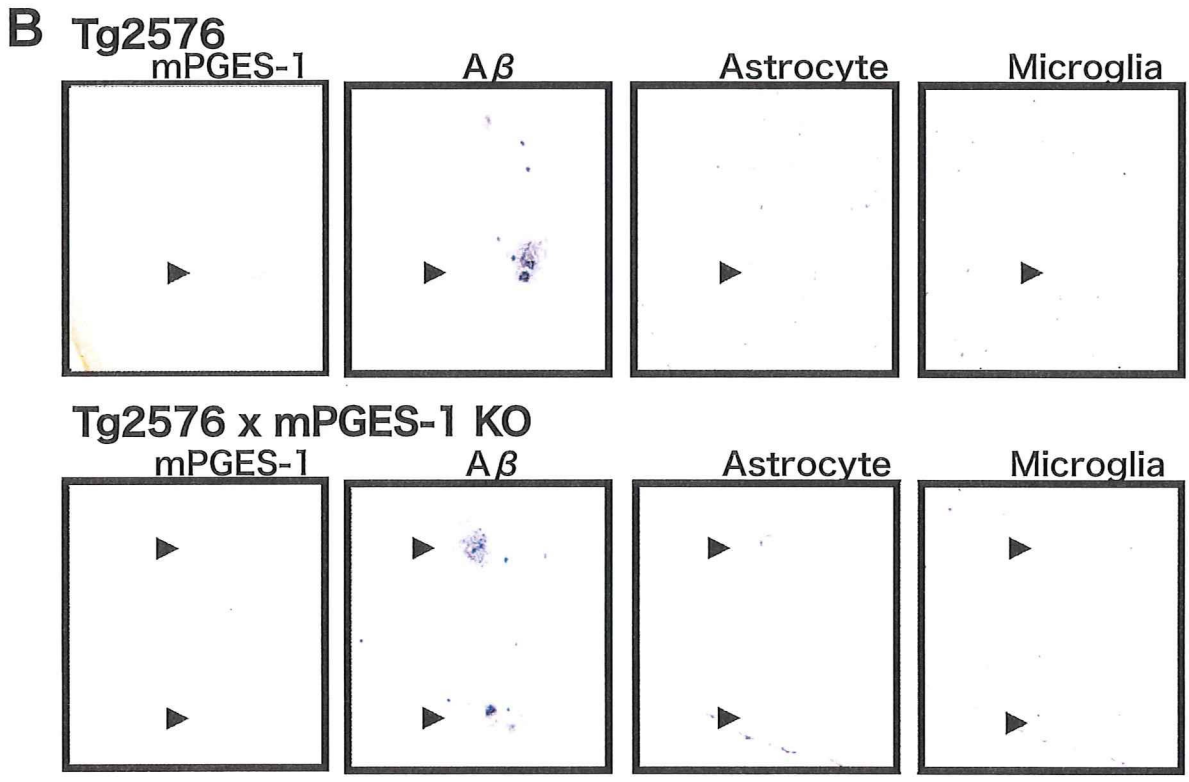
B
Tg2576
mPGES-1
Aβ
Astrocyte
Microglia
Tg2576 x mPGES-1 KO
mPGES-1
Aβ
Astrocyte
Microglia

Fig. 5